Research article

X-RAY SPECTROMETRY

Received: 20 November 2015 Revised: 11 December 2015 Accepted: 13 December 2015 Published online in Wiley Online Library

(wileyonlinelibrary.com) DOI 10.1002/xrs.2680

Analysis of the spectacular gold and silver from the Moche tomb 'Señora de Cao'

R. Cesareo,[a,e]* R. Franco Jordan,[b] A. Fernandez,[b] A. Bustamante,[c] J. Fabian,[c] S. del Pilar Zambrano,[c] S. Azeredo,[d] R. T. Lopes,[d] G. M. Ingo,[e] C. Riccucci,[e] G. Di Carlo[e] and G. E. Gigante[f]

On the north coast of present-day Peru, between the Andes and the Pacific Ocean, approximately between 100 and 600 AD, the Moche civilization prospered. The Moche were very sophisticated artisans and metal smiths, so that they are considered the finest producers of jewels and artifacts of the region. Their metalworking ability was impressively demonstrated by the excavations of the tomb of the 'Lady of Cao' (dated around third–fourth century AD) discovered by Regulo Franco in 2005. Impressive is the beauty of the artifacts, and also the variety of metallurgical solutions, demonstrated by not only the presence of objects composed of gold and silver alloys but also of gilded copper, gilded silver, and tumbaga, a poor gold Cu-Au alloy subject to depletion gilding.

About 100 metal artifacts from the tomb of the Lady of Cao, never before analyzed, were studied by using various portable equipments based on following non-destructive and non-invasive methods:

- energy-dispersive X-ray fluorescence with completely portable equipments;
- transmission of monenergetic X-rays;
- radiographic techniques; and
- optical microscopy.

Gold objects and gold areas of nose decorations are characterized by approximately the same composition, that is, *Au* = (79.5 ± 2.5) %, *Ag* = (16 ± 3) %, and *Cu* = (4.5 ± 1.5) %, while silver objects and silver areas of the same nose decorations show completely erratic results, and a systematic high gold concentration. Many gilded copper and tumbaga artifacts were identified and analyzed. Further, soldering gold–silver was specifically studied by radiographs.

Additional measurements are needed, particularly because of the suspect that depletion gilding was systematically employed also in the case of some nose decorations. Copyright © 2016 John Wiley & Sons, Ltd.

Introduction

Historical and geographic introduction

On the north coast of present-day Peru (Fig. 1) approximaterly between 1200 BC and 1375 AD, various relevant civilizations flourished: Cupisnique (1200–200 BC) Chavín (1000–200 BC), Vicús and Frías (200 BC–300 AD), Moche (100–600 AD), and Sicán (700–1375 AD).

Among them, the most important, from the point of view of metallurgical ability, was the Moche civilization (also called Mochica).

The Moche civilization flourished in areas south of the Vicús, in the Moche and Chicama valleys, where its great ceremonial centers have been discovered, producing painted pottery, monuments, and gold ornaments. The Vicús and Moche cultures thrived within a relatively short distance of each other. The Moche were known as sophisticated metal smiths, both in terms of their technology, and the beauty of their jewels.

The Moche metalworking ability was impressively demonstrated when Walter Alva and coworkers discovered in 1987 the 'Tumbas Reales de Sipán'[1,2] and, more recently, when Regulo Franco Jordan discovered the tomb of the 'Lady of Cao' in 2005 (Fig. 2).[3–6] Spectacular gold and silver funerary ornaments were excavated and are now exposed in the Museum 'Tumbas Reales de Sipán' in Lambayeque, close to Chiclayo and in the site Museum of Cao, about 60 km north to Trujillo.

Previously, in the late 1960, tombs rich of metals attributed to the Moche were discovered and looted in an area that came to be known as Loma Negra, in the Vicús region. Hundreds of objects attributed to Loma Negra were sold to US collectors and finally partially transferred to the Metropolitan Museum of New York.[7,8] The site of Loma Negra was dated about second–third century AD,possibly before the tombs of the Lady of Cao (~300 AD) and of the lord of Sipán (~350 AD). However, these dates are uncertain.

* *Correspondence to: Roberto Cesareo, Istituto di Matematica e Fisica, Università di Sassari; via Nulauro 3, 07041 Alghero, Italy. E-mail: cesareo@uniss.it*

a *Dipartimento di Matematica e Fisica, Università di Sassari, Sassari, Italy*

b *PACEB Museo Cao (Fundación Wiese), Trujillo, Peru*

c *Universidad Nacional Mayor de San Marcos, Lima, Perù*

d *COPPE, Universidade Federal do Rio de Janeiro, Rio de Janeiro, Brasil*

e *Istituto per lo studio dei materiali nano strutturati, CNR-Montelibretti, Rome, Italy*

f *Dipartimento di Scienze di base ed applicate per l'ingegneria, Università di Roma 'La Sapienza', Rome, Italy*

Figure 1. Region of the Moche civilization in the north of present-day Peru around Chiclayo, Trujillo, and the Andes, and between the Andes and the Pacific, for an approximate area of 150 000 Km^2. The tomb of the Lady of Cao is located in the 'Complejo El Brujo' (courtesy of Fundacion Wiese).

Analytical introduction

Nothing was analysed before from the treasure of the tomb of the Lady of Cao, but several analytical studies were carried out on other Moche precious artifacts.

Fragments from Moche civilization's objects and more specifically from Sipán alloys were analyzed by using various destructive techniques;[7–17] some general information could be deduced from all these measurements:

- moche metalworking was based primarily upon objects made of hammered sheet metal;
- besides native gold and native gold–silver alloys (with some copper), gold and silver were already intentionally alloyed at that time; and
- the Moche developed very low carat gold or silver alloys appearing from outside as silver or gold by depleting the surface from copper; this process of depletion gilding was called 'tumbaga' by the Spanish conquerors,and is a known technique, which was used in many cultures worldwide, as early as the third millennium BC in Mesopotamia.[18] In the Moche case, the low carat alloy was burned and/or treated with acids extracted from plant juices, which produced a copper oxide that could be removed mechanically. The object was then placed in an oxidizing solution containing, it is believed, salt, and ferric sulfate. This process removed through oxidation the silver from the surface of the object leaving only gold. In the following the term, tumbaga will be used for a poor-gold Au Cu-Ag-alloy subject to depletion gilding.

A relevant number of artifacts, mainly made from gilded or silvered copper sheets, but also on gold, silver, gold–silver, and silvered gold from Loma Negra, were accurately studied and analyzed by Deborah Schorsch by employing energy dispersive X-ray fluorescence (EDXRF) attached to a scanning electron microscope and wave dispersive X-ray Spectrometry.[8] The gold objects from Loma Negra showed following average composition: Au ~ 80%, Ag = 10–20%, and Cu = 5–15%. The analyzed silver objects showed a high Ag-content, of about 97–99%. Copper covers the difference from 100%, and no gold was registered in these silver objects.

Further, fragments from 17 Moche objects on copper, silver alloys, and gold alloys from the Museum 'Tumbas Reales de Sipán' have been analyzed by Gerhard Hörz and Monika Kallfass,[9,10]

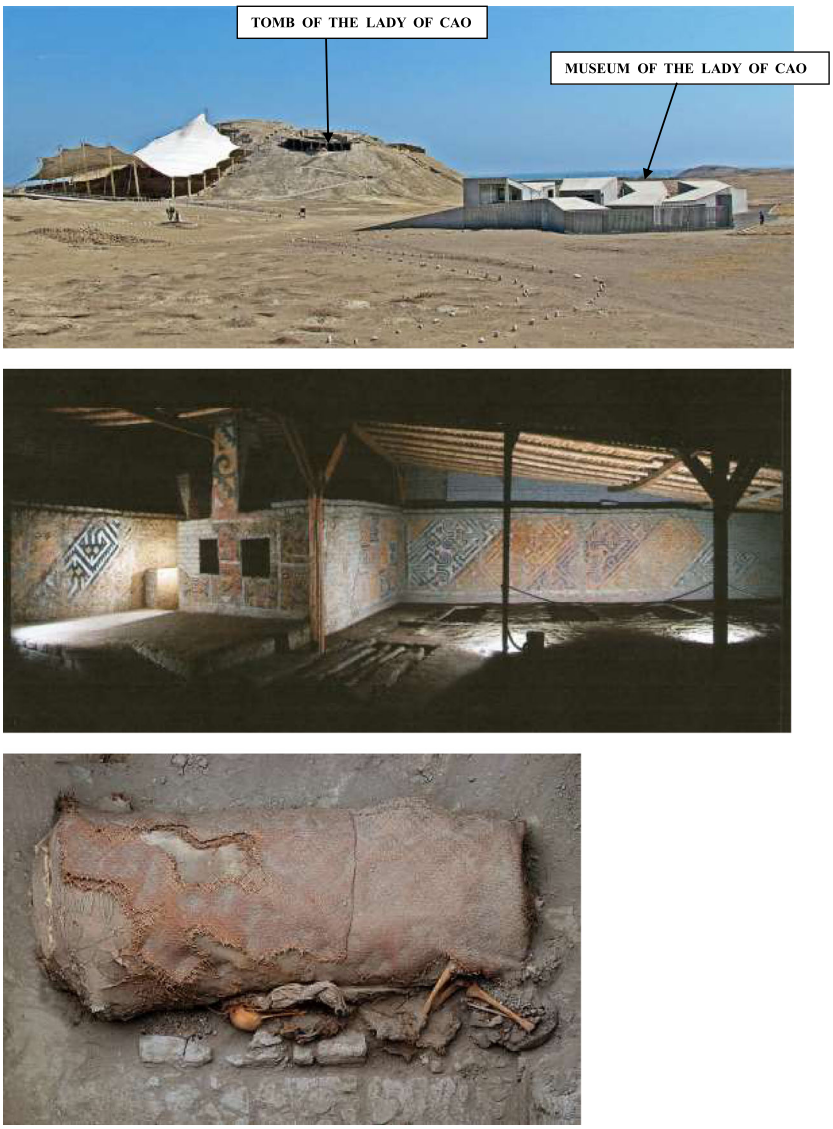

Figure 2. View of the 'pyramid' excavations (top figure), tomb of the 'Lady of Cao' (middle) and sarcophagus of the Lady of Cao. The pyramid is located in the 'Complejo El Brujo', several hundreds of meters from the Pacific Ocean, and a few kilometer from Magdalena de Cao, which is about 60 km north from Trujillo (Courtesy of Fundacion Wiese).

using optical emission spectrometry with inductively coupled high frequency plasma, wavelength-dispersive spectrometry, and structural analysis. These authors were able to distinguish various techniques of manufacture (working, casting, gilding, depletion silvering, embossing, and depletion gilding); in particular, they were able to identify the following:

- gilded copper objects: a series of objects found in the tomb of the 'Señor de Sipán' was identified as made of gilded copper, characterized by a thin gold film (2–6 μm). The coatings consist of a gold–copper alloy containing some silver;
- copper–silver alloys: fragments from several human head shapes beads have been analyzed, made of a sheet composed of 79% Cu, 20% Ag, and 1% Au approximately;
- copper–gold–silver alloys (depletion gilding objects): fragments were analyzed from a headdress, a chin ornament, an ornamental disc, and ornamental beads; the average composition of the headdress was calculated to be 60% Cu, 34% Au, and 6% Ag. The average composition of the chin ornament is 40% Cu, 50% Au, and 10% Ag; the average composition of the ornamental disc is 30% Cu, 60% Au, and 10% Ag, and the average composition of the ornamental bead is 20% Cu, 65% Au, and 15% Ag. It should also be observed that the alloy composition is strongly dependent on the distance from the surface (Fig. 3).

Recently, Carole Fraresso[19] has examined 15 fragments from the Moche site of Huaca de la luna and Huaca del sol. From the analysis of these fragments by an EDXRF-system associated to a scanning electron microscope, ten were on nearly pure copper, and one is possibly on tumbaga; because of the surface Au enrichment, another is composed of 98% Cu, 1.5% Au, and 0.5% Ag. The two others seem to be on gilded copper.

It is evident from all measurements carried out and from the variety of object composition that the analytical problems of Moche metallurgy are extremely complicated, because of the variety of

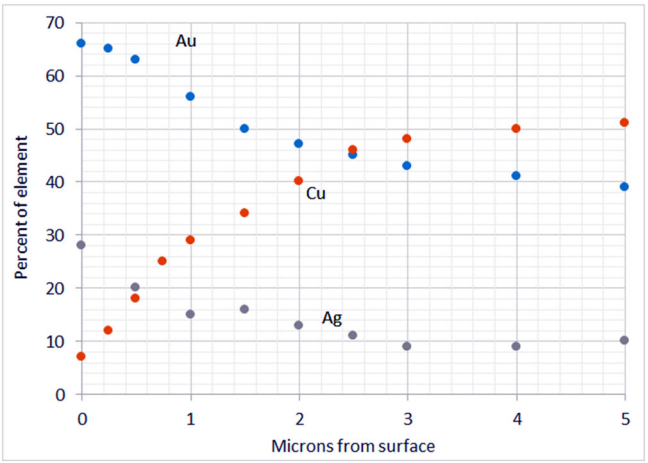

Figure 3. Examples of tumbaga. The mean profiles are shown of the concentrations of Cu, Au, and Ag *versus* distance from the surface, for four fragments of Moche artifacts. The Au concentration decreases while the Cu-concentration increasing *versus* depth. Modified from G. Hörz and M. Kallfass (Ref. 8).

alloys and manufacture techniques, of the long time burial and of layered structure of others.

References[20–37] are suggested to better understand the metallurgy of pre-Hispanic cultures from the north of Peru.

Experimental

Energy dispersive X-ray fluorescence

Characteristics and experimental set-up

Energy dispersive X-ray fluorescence analysis is able to quantify the composition of a gold, silver, or copper alloy by using, for example, standard samples of the same alloys (Section *Quantitative analysis of gold and silver alloys*). EDXRF-analysis is also able to detect, and qualitatively determine trace elements, when approximately present a level of 0.1% or more. EDXRF is a surface analysis, in the sense that the thickness of the alloy involved in the analysis is of the order of microns to a maximum of tens of microns (Figs 11 and 12); the results are therefore related to this depths and are generally valid in absence of surface enrichment phenomena (patina and ions migration processes).

For the measurements carried out in the Museum of Cao, the portable equipment was composed of a mini X-ray tube by AMPTEK (Bedford, MA, USA),[38] which is characterized by a Ag-anode and works at 40 kV and 200 μA maximum voltage and current, and a 123-Si-drift detector.[39] Bias supply and electronics of both X-ray tube and detector are located in the case of tube and detector, respectively; in such a manner, the equipment is extremely compact (Fig. 4).

The Si-drift is a thermoelectrically cooled detector, with a 450-μm and 7-mm^2 thickness and area of the Si-crystal respectively, and a thin Be-window, of typically 12.5-μm thickness (0.5 mil) with about 125-eV energy resolution at 6.4 keV.[38] This detector has an efficiency of 97%, 39%, and14% at 10, 20, and 30 keV, respectively. The irradiated and analyzed area is of about 20 mm^2, when the object is at a distance of a few centimeters.

The X-ray beam intensity with a not collimated and not filtered X-ray tube is largely in excess for analysis of alloys. For this reason, the X-ray beam is collimated and filtered, also to better its 'form',

Figure 4. Energy-dispersive X-ray fluorescence portable equipment, composed of a Si-drift detector (on the right; 123SDD: 450-μm thickness, 7-mm^2 area, and 125-eV energy-resolution at 5.9 keV) and a Ag-anode X-ray tube (40 kV, 100-μA maximum voltage and current) (38). Electronics including bias supply and Multi-Channel Analyzer (MCA) are in the case of the detector; X-ray tube bias supply is in the case of the X-ray tube. A typical measurement takes 50–100 s. The energy-dispersive X-ray fluorescence-equipment is analyzing the crown PACEB-F4-00069.

and to partially monochromatize the X-ray beam. The object to be analyzed is positioned at 1.5–3-cm distance from both X-ray tube and detector. The measuring time ranges from about 50 s to about 200 s, mainly according to the sample composition and size.

Standard gold and silver alloys were employed for calibration and for quantitative determination of alloy composition, containing known concentration of gold, silver, and copper (gold alloys) and of silver, copper, and gold (silver alloys). As will be shown and explained later, the ratios Cu/Au and Ag/Au were employed for calibration.

To measure gilding thickness of gilded copper or silver, the Cu ($K\alpha/K\beta$)-ratio or Ag($K\alpha/K\beta$)-ratio and the (Au-L_a/Cu-K_a) or (Au-L_a/Ag-K_a)-ratios were employed. Further, commercial gold leaves were employed (each Au-foil 0.125 μm thick) to simulate gilded copper or tumbaga, and silver foils (each Ag-foil 0.25 μm thick) to simulate the 'silvered copper' or 'Ag-tumbaga'. Also calibrated Au-leaves were employed, and several gilded-copper samples with calibrated gilding thickness. Thick sheets of pure copper and silver were also employed.

X-ray spectrum of gold alloys

The final result of EDXRF – analysis of a sample is a X-ray spectrum containing a set of X-lines for each detectable element present in the analyzed object.

When K-shells are excited, four characteristic lines are emitted by each element: $K\alpha_1$, $K\alpha_2$, $K\beta_1$, and $K\beta_2$.[40,41] When L-shells are excited, nine characteristic lines are emitted by each element, that is, in order of energy, $L\eta$, $L\alpha_1$, $L\alpha_2$, Ll, $L\beta_1$, $L\beta_2$, $L\beta_3$, $L\gamma_1$, and $L\gamma_3$.[40,41]

From a practical point of view, and because of the finite energy-resolution of semiconductor detectors, the line combinations Ka_1–Ka_2, coincide in a unique peak, and the same happens for the lines pairs or triplets $K\beta_1$ –$K\beta_2$, $L\alpha_1$–$L\alpha_2$, and $L\beta_1$–$L\beta_2$–$L\beta_3$. K-lines are therefore identified by two X-rays $K\alpha$ and $K\beta$, and L-lines by six X-rays $L\eta$, $L\alpha$, Ll, $L\beta$, $L\gamma_1$ and $L\gamma_3$ of which only $L\alpha$ and $L\beta$ of high intensity.

By analyzing a gold alloy, containing Au-Ag-Cu, and using a proper filter at the X-ray tube output to attenuate the low-energy part of the spectrum, a typical X-ray spectrum is obtained, as shown in Fig. 5.

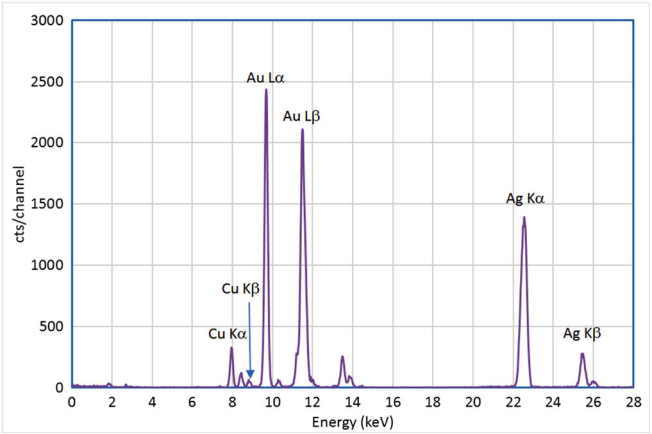

Figure 5. X-ray spectrum of an Au-Ag-Cu alloy (70% Au, 25% Ag, 5% Cu), obtained with the equipment shown in Figure 4; the X-ray tube was working at 35 kV and 30 μA. The X-ray peaks are, from leftf: Cu-Kα line (8 keV), Au-Ll (8.5 keV), Cu-Kβ (8.9 keV), Au-Lα (9.7 kev), Au-Lη (10.3 keV), Au-Lβ (11. keV), Au-Lγ (13. keV), Ag-Kα (22 keV), and Ag-Kβ (25 keV). Au X-rays have the following relative intensity: Au-Ll (5), Au-Lα (100), Au-Lη(2.3), Au-Lβ(135), and Au-Lγ (25).

Quantitative analysis of gold and silver alloys

Artifacts of very different size composition and form were analyzed. It is, therefore, very difficult to reproduce a fixed geometrical arrangement and, in particular, to have always the same distances X-ray tube object detector. For these reasons, there was a preferred approach for quantitative analysis, of using, instead of the intensity of X-rays emitted by an element, the intensity ratio of two components (for example Cu/Au and Ag/Au), which is not depending on the geometry.

In the case of gold or silver alloys, composed by Au-Ag-Cu and Ag-Cu-Au respectively, and assuming that Au(%) + Cu(%) + Ag(%) = 100 (both for Au and Ag-alloys), by plotting the ratios $(\text{Cu-K}\alpha/\text{Au-L}\alpha)_{\text{counts}}$ *versus* $(\text{Cu-K}\alpha/\text{Au-L}\alpha)_{\text{concentration}}$, $(\text{Ag-K}\alpha/\text{Au-L}\alpha)_{\text{counts}}$ *versus* $(\text{Ag-K}\alpha/\text{Au-L}\alpha)_{\text{concentration}}$ and the same for Ag-alloys, it turns out that there is approximately a linear relationship, at least for Ag-concentrations in Au up to about 30%, Cu-concentrations in Au up to 20%, for Au-concentrations in Ag up to 30%, and Cu-concentrations in Ag up to 20%.

When other elements are present as trace elements, their concentrations can be determined by using the method of fundamental parameters.

Errors, uncertainties, and minimum detection limits related to quantitative analysis of gold and silver alloys by EDXRF-analysis will be discussed in the following.

Kα/Kβ or Lα/Lβ-ratios

The Kα/Kβ and Lα/Lβ-ratios for all elements have been calculated and, in several cases, were measured[42–46] (Fig. 6). Theoretical values are calculated for infinitely thin samples, that is, when secondary interactions in the sample are negligible. The ratios Kα/Kβ and Lα/Lβ can largely vary

- when the considered element is not 'infinitely thin' (self-attenuation effect); and
- when a layer of a different material is covering the considered element.

This is the case of gildings, silverings, tumbagas of all type, which are extremely common in the Moche metallurgy.

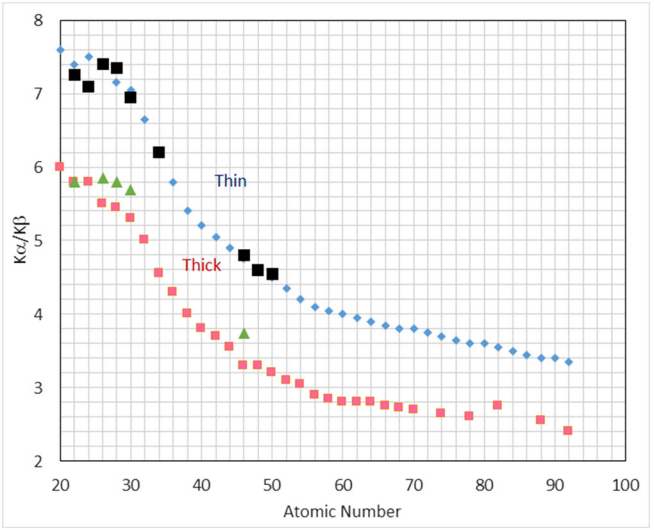

Figure 6. Average Kα/Kβ ratio *versus* atomic number *Z*, for infinitely thin (blue rhombs) and thick (red squares) single element samples when the exciting energy is much higher than Kdiscontinuity; values were deduced from various calculations. Experimental results are also shown (thick samples: green triangles; thin samples, black squares). An error of about ±0.2 may be assumed for thin samples, a lower error for thick samples.

Self-attenuation effects on Kα /Kβ and Lα /Lβ-ratios

For a mono-elemental sample of any thickness, (not infinitely thin), self-attenuation effects must be considered, that is, the different attenuation of Kα and Kβ X-rays (or Lα and Kβ X-rays) emitted by the element in a point of the sample and attenuated by the element itself.

Kα/Kβ and Lα/Lβ X-rays vary according to following equations[38–42]:

$$\frac{K_\alpha}{K_\beta} = \left[\left(\frac{K_\alpha}{K_\beta}\right)_{\text{thick}} \Big/ \left(\frac{K_\alpha}{K_\beta}\right)_{\text{thin}}\right] \left(\frac{1-e^{-(\mu_0+\mu_1)\,d}}{1-e^{-(\mu_0+\mu_2)\,d}}\right) = \left(\frac{\mu_0+\mu_2}{\mu_0+\mu_1}\right) \left(\frac{1-e^{-(\mu_0+\mu_1)\,d}}{1-e^{-(\mu_0+\mu_2)\,d}}\right) \quad (1)$$

$$\frac{L_\alpha}{L_\beta} = \left[\left(\frac{L_\alpha}{L_\beta}\right)_{\text{thick}} \Big/ \left(\frac{L_\alpha}{L_\beta}\right)_{\text{thin}}\right] \left(\frac{1-e^{-(\mu_0+\mu_1)\,d}}{1-e^{-(\mu_0+\mu_2)\,d}}\right) = \left(\frac{\mu_0+\mu_2}{\mu_0+\mu_1}\right) \left(\frac{1-e^{-(\mu_0+\mu_1)\,d}}{1-e^{-(\mu_0+\mu_2)\,d}}\right) \quad (2)$$

where

- thick and thin represent the tabulated and/or measured ratios for infinitely thick and thin samples,
- μ_0 is the linear attenuation coefficient (in cm^{-1}) of the considered element at mean energy E_0,[47]
- μ_1 is the linear attenuation coefficient (in cm^{-1}) of the considered element, at the energy of its Kα (or Lα) line,
- μ_2 is the linear attenuation coefficients (in cm^{-1}) of the considered element, at the energy of its Kβ (or Lβ) radiation, and
- -d represents the thickness (in cm) of the sample.

Eqns (1) and (2) are valid when both incident and output beam are normal to the sample surface, and for pure elements; otherwise, the material composition must be taken into account.

The values of Eqns (1) and (2) were normalized to 1, in such a manner that Kα/Kβ (or Lα/Lβ)-ratios = 1 for thin samples.

Figure 7 shows, for example, the self-attenuation curves for Au.

Kα /Kβ (or Lα /Lβ)-ratios of X-rays emitted by an element in an internal sheet and attenuated by the external sheet (or sheets)

When a sheet, supposed thick, composed by a single element, (or containing this element), is covered by a sheet of another element, (or containing this element), then the ratios (Kα/Kβ) or (Lα /Lβ) are altered in the following manner because of the different attenuation of the Kα and Kβ X-rays (or Lα and Kβ X-rays) of the first element[42,48] (Fig. 8):

$$\frac{K_\alpha}{K_\beta} = \left(\frac{K_\alpha}{K_\beta}\right)_{thick} e^{-(\mu_1-\mu_2)d} \quad (3)$$

$$\frac{L_\alpha}{L_\beta} = \left(\frac{L_\alpha}{L_\beta}\right)_{thick} e^{-(\mu_1-\mu_2)d} \quad (4)$$

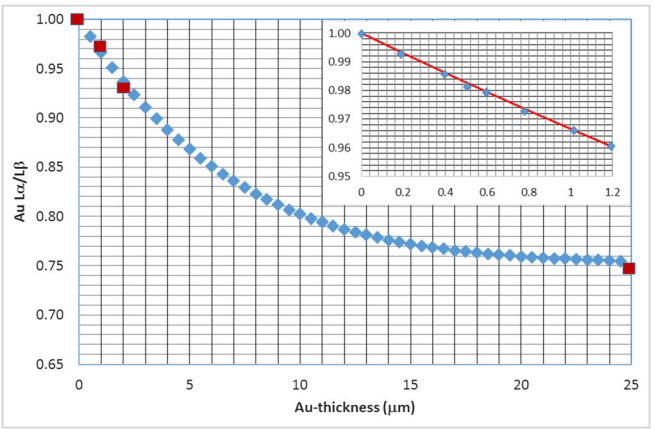

Figure 7. Self-attenuation effect of Au-L lines in the case of gildings, according to Eqn (2) (blue rhombs). Red squares refer to experimental measurements. The behavior for low Au-thickness is shown in the square on the top right.

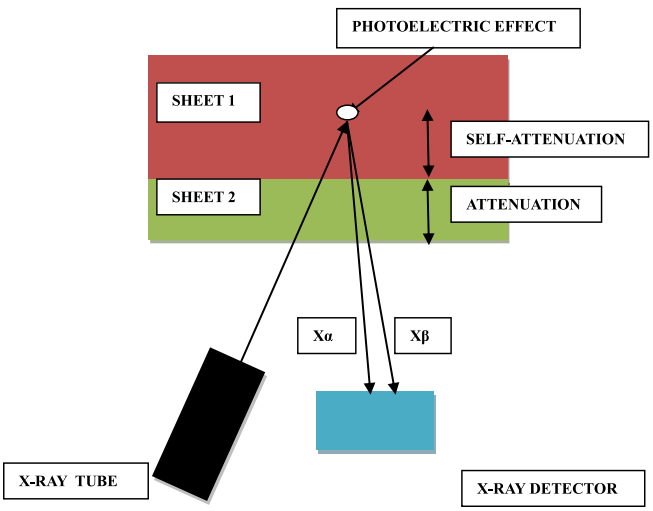

Figure 8. Photoelectric effect and emission of X-rays (Xα and Xβ), which self-attenuated in the first sheet (Eqns 1 and 2), are attenuated in the second sheet (Eqns 3 and 4) .

where

Kα/Kβ and Lα/Lβ are the ratios of the X-rays of the most internal sheet, supposed on infinite thickness,

μ_1 represents the linear attenuation coefficient of the second sheet at the energy of Kα (or Lα) radiation of the first sheet,[47] and

μ_2 is the linear attenuation coefficient of the covering sheet at the energy of the Kβ (or Lβ) radiation of the internal sheet.

The behavior of copper covered by gold is shown in Fig. 9.

Ratio of X-rays of elements in the external to an element in the internal sheet

Another way to experimentally determine the thickness of the external elemental sheet from the X-ray spectrum, assuming that the internal elemental sheet has an infinite thickness consists in the direct use of the X-ray ratio of the two elements characterizing the two sheet (for example, in the case of gilded copper, the ratio Au-Lα/Cu-Kα). By defining a and b, the external and internal sheet of the following equation, may be written[48]:

$$\frac{Nb}{Na} = P[1 - e^{-(\mu_{b0}+\mu_{b1})}]e^{-(\mu_{b0}+\mu_{b2})}d \quad (5)$$

where

- P is a parameter to be determined from experimental measurements,
- μ_{b0} represents the linear attenuation of the element of sheet b at incident energy E_0,
- μ_{b1} represents the linear attenuation of the element of sheet b at energy of Kα-line of element a, and
- μ_{b2} represent the linear attenuation of the element of sheet b at energy of Kβ-line of element a.

Figure 10 shows the curves described by Eqn (5) for gilded copper.

This described method based on the use of Kα/Kβ (or Lα/Lβ)-ratios and of the ratio of X-rays of elements from contiguous layers was also employed by various authors.[42,49–52]

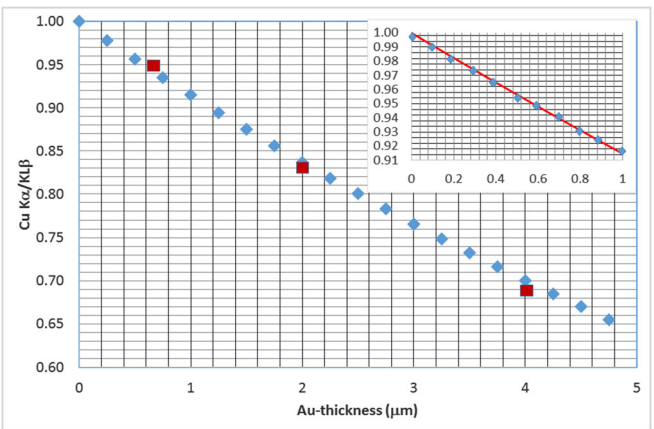

Figure 9. Cu (Kα/Kβ)-ratio *versus* Au-thickness, according to Eqn (3); theoretical and experimental values are shown with blue rhombs and red squares respectively. The behavior for low Au-thickness is shown in the square on the top right.

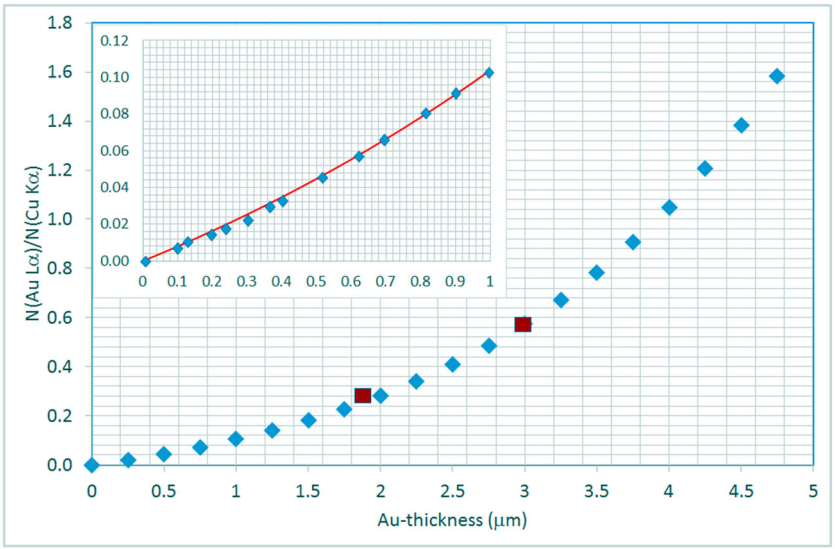

Figure 10. Au-Lα/Cu-Kα-ratio *versus* Au-thickness according to Eqn (5); theoretical and experimental values are shown with blue rhombs and red squares, respectively. The behavior at low thickness values is shown in the square on the left top.

Reliability, uncertainties, and errors associated to energy-dispersive X-ray fluorescence analysis of gold and silver alloys

Reliability, uncertainties, and errors related to EDXRF-analysis of gold and silver artifacts depend on many factors: the artifact itself (method of production, composition, use, possible restoration and conditions)[53–59], the equipment and its use, with special reference to the X-ray detector, the calibration samples, the X-ray spectrum with special reference to the width of X-ray peaks and counting statistics, reference samples for EDXRF-analysis, and finally data processing.

Considering all these factors, following absolute errors may be considered reasonable.Gold alloy, gold: ± (1–2)%; silver: ± (0.5–2)%; copper: ± (0.5–1)%; Silver alloy, silver: ± (1–2)%; copper: ± (0.5–1)%; gold: ± (0.5–1.5)%; Copper alloy, copper: ± (1–2)%

$$\text{Thickness deduced by means of Cu}(K\alpha/K\beta)\ \text{-ratio} : \pm(0.5-1)\ \mu\text{m}$$

$$\text{Thickness deduced by means of Au}(L\alpha/L\beta)\ \text{-ratio} : \pm(0.3-1.5)\ \mu\text{m}$$

$$\text{Thickness deduced by means of AuL}\ \alpha/\text{CuK}\ \alpha\ \text{-ratio} : \pm(0.2-1)\ \mu\text{m}$$

Transmission measurements

As observed previously, EDXRF analysis is a technique, which analyzes a thin surface layer. In the case of metals such as gold and silver, it typically interests a depth of microns up to a maximum of tens of microns (Figs 11 and 12). Therefore, EDXRF is affected by a large indetermination when the sample composition is altered because of surface enrichments processes, as often happens in the case of silver alloys, and sometimes in the case of gold alloys.

An alternative technique of volume analysis was therefore developed,[60,61] which employs the same equipment of EDXRF-analysis; by monochromatizing the X-ray beam by means of a secondary target composed of a proper element, the attenuation

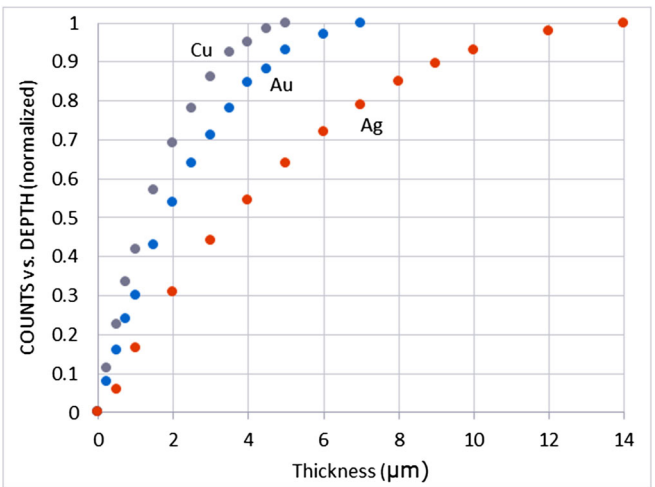

Figure 11. Typical depths involved when an X-ray beam of about 30-keV average energy irradiates a gold alloy (*Au* = 75%, *Ag* = 20%, *Cu* = 5%), and fluorescent X-rays are emitted. The percentage of radiation coming from each depth is shown, indicating, for example, that about 70% of the Au-Lα, Ag-Kα, and Cu-Kα X-rays are originating from the first 3 μm (Au), 5.5 μm (Ag), and 2 μm (Cu) of the Au-sample, respectively.

of K-X rays emitted by this element can be employed to determine thickness of a sample when composition is known, or composition (for two or three components alloy) when thickness is known or measured.

Theoretical background

The attenuation of single Kα and Kβ-lines emitted by target element *b* can be employed to determine the thickness of sheet *a*. For example, a secondary target of Sn was usefully employed to determine thickness and/or composition of Au and Ag alloys. In this case, the following may be written concerning attenuation of Sn-Kα and Sn-Kβ lines:

$$\text{Sn}[K\alpha]/\text{Sn}[K\alpha]_0 = \exp\left(-\mu_{a\alpha}\, d_a\right) \text{ and} \qquad (6)$$

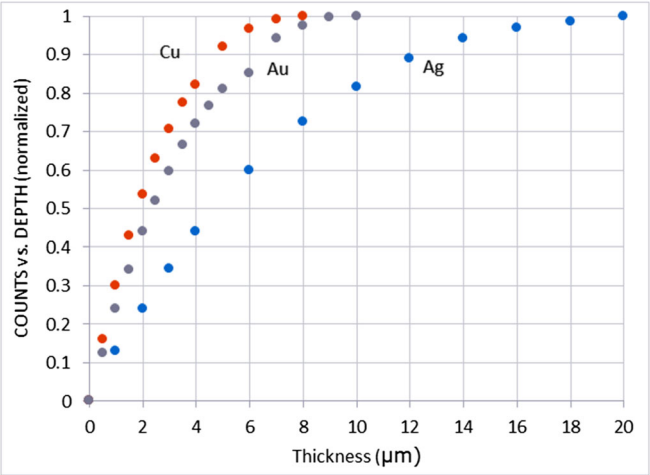

Figure 12. Typical depths involved when a X-ray beam of about 30-keV average energy irradiates a silver alloy (*Ag* = 70%, *Cu* = 15%, *Au* = 15%, *Cu* = 15%), and fluorescent X-rays are emitted. The percentage of radiation coming from each depth is shown indicating, for example, that about 70% of the Ag-Kα, Cu-Kα, and Au-Lα X-rays are originating in the first 8 μm (Ag), 3 μm (Cu), and 4 μm (Au) of the Ag-sample, respectively.

$$\mathrm{Sn[K\beta]/Sn[K\beta]_0} = \exp\left(-\mu_{\beta_\alpha} d_a\right) \tag{7}$$

where $[K\alpha]_0$ and $[K\beta]_0$ indicate Kα and Kβ values of element *b*, with no element *a*.

When sample *a* is composed by a two components alloy (for example, Ag-Cu or Au-Ag), then, the following system of equations can be contemporaneously written:

$$\mathrm{Sn[K\alpha]/Sn[K\alpha]_0} = e^{-95\ d(Ag)} \cdot e^{-150\ d(Cu)} \tag{6'}$$

$$\mathrm{Sn[K\beta]/Sn[K\beta]_0} = e^{-425\ d(Ag)} \cdot e^{-107\ d(Cu)} \tag{7'}$$

Each of the Eqns (6′) and (7′) can be employed to determine the thickness of the sheet.

Alternatively, when the thickness of the two components alloy is known or can be measured and has a value approximately less than 1 mm for silver alloys, and less than 100 μm for gold alloys, then Eqns (6′) and (7′) can be employed to approximately determine the alloy composition.

That gives the possibility to check, with a simple volume analysis based on transmission of monoenergetic X-rays, the analytical results from EDXRF-analysis, which are related to a thin depth, and can be, therefore, affected by surface enrichments processes, which alter the surface composition and, therefore, in many cases, the reliability of EDXRF-analysis.

Experimental set-up and calibration

The experimental set-up for transmission measurements includes the same X-ray tube and detector employed for EDXRF-analysis and described previously, that is, a Ag-anode X-ray tube working at 40-kV and 200-μA maximum voltage and current and a Si-drift X-ray detector. The photons emitted by the X-ray tube are filtered, collimated, and irradiate the Sn-target, producing by photoelectric effect Sn-K X-rays (with energy of 25.2 and 28.5 ke,V respectively). The Ag or Au-sheets to be measured are inserted between the Sn-target and the detector entrance.

Calibration curves from Eqn (6′) are shown, for example, in Fig. 13. Results of transmission measurements can be compared with the results of EDXRF-analysis and are a test of its reliability in the case of possible surface enrichments.

Radiography

X-ray radiography is an imaging method that uses X-rays to reveal the structure of an object based on the different densities of its constituent materials. In the case of the objects from the tomb of the Lady of Cao, we should consider the fact that the large majority of the objects are sheets basically on gold or silver alloys and the approximate thickness was measured to be about 100 μm for Au-layers and 200–300 for Ag-layers.

Radiographs were carried out with the following portable equipment (Fig. 14):

- a portable mini X-ray tube by AMPTEK, working at 50 kV and 100 μA maximum voltage and current;
- a flat panel detector by Schick Technologies; and
- Image analysis software ISEE.

To image the Moche jewels under study the equipment worked at 25, 35, 45 and 50 kV. The first value appeared to be ideal to visualize the Ag-areas, while the last values (45 and 50 kV) were able to image the gold areas.

Optical microscopy

Optical microscope investigations were carried out by using a Wild MB (Heerbrugg, Heerbrugg Switzerland) optical microscope equipped with a Leica DFC 320 digital camera.

The following nose decorations were observed by optical microscopy:

- -nose decoration Proyecto Arqueológico Complejo El Brujo (PACEB)-F4-00002

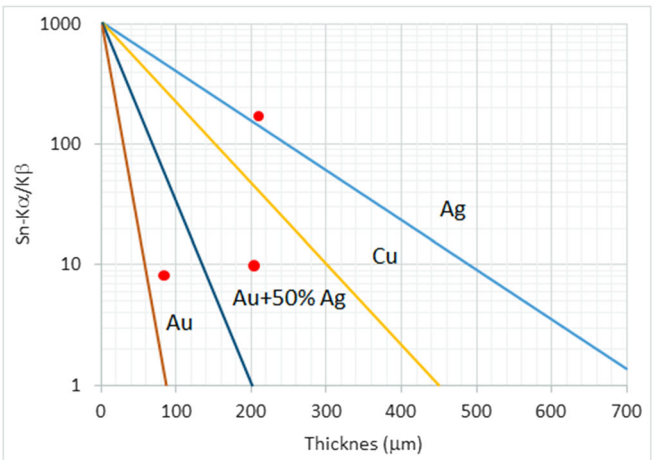

Figure 13. Transmission measurements: Sn-Kα/Sn-Kα° *versus* thickness (in μm) for absorbers with various thicknesses and for (from left) Au, Au + 50%Ag, Cu, and Ag. Red circles refer (from left) to gold area of object F4-0002, to silver area of object F4-0060 and to silver area of object F4-0002 (blue line).

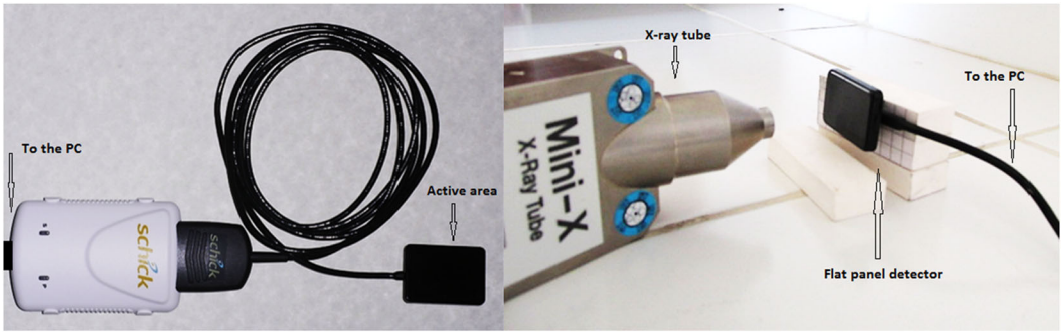

Figure 14. Flat panel-detector employed for the radiographs at the Museum of the Lady of Cao (left). Experimental set-up for digital radiography image acquisition including X-ray tube and digital detector is shown on the right.

Results on the artifacts from the tomb of the Lady of Cao

Gold

Energy-dispersive X-ray fluorescence analysis

Forty one nose decorations partially on gold and partially on silver were analyzed. (Figures 15–17).[62] The composition of the gold area is shown in Table 1 and Au-Ag-Cu distribution in Fig. 18. It appears clear, and not casual, that gold areas of nose decorations have same composition.

Figure 15. Front and rear side of the nose decoration PACEB-F4-0002. It is composed of a body on laminated gold alloy with two shields (on the front side) and two huts on almost pure silver superimposed and glued. T and t indicate areas where transmission measurements were carried out, numbers 1-6 and a-h EDXRF-measurements carried out in 2014 and 2015, respectively. The red vertical line indicates the radiographic profile shown in Fig. 20. Gold alloy composition: $Au = 74.5\%$, $Ag = 19.5\%$, $Cu = 5.5\%$. Silver alloy composition: $Ag = 99.2\%$, $Cu = 0.02\%$, $Au = 0.8\%$.

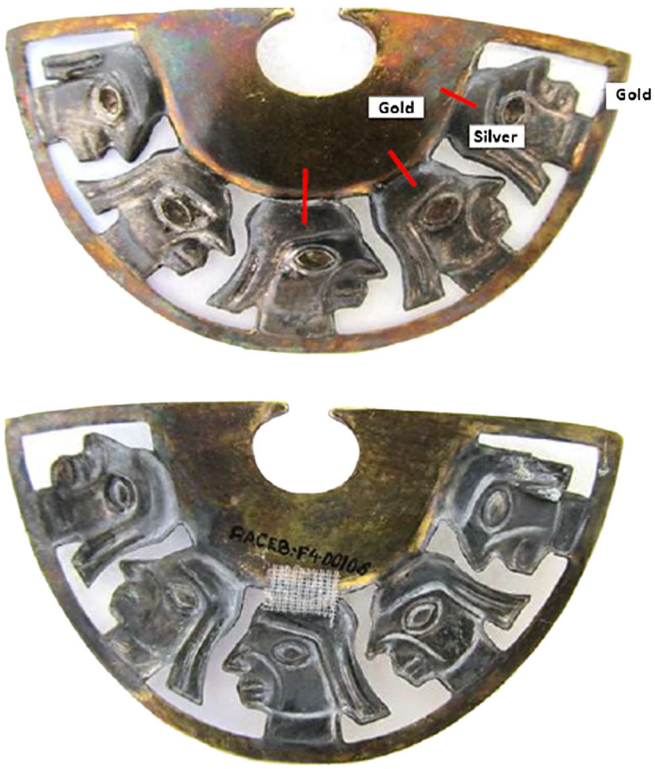

Figure 16. Front and back side of nose decoration PACEB-F4-00106. Upper half-crown and lower half-crown strip are on gold alloy. The five heads are on silver alloy and are soldered to the half-crown at the top, and to the strip at the bottom. Red lines show the position of quantitative grey-value curves from radiographs (Figs 21 and 22). Gold alloy composition: $Au = 81.2\%$, $Ag = 17.7\%$, $Cu = 1.1\%$. Silver alloy composition: $Ag = 91.8\%$, $Cu = 4\%$, $Au = 4.2\%$.

Also 16 artifacts completely on gold were analyzed, which results are reported in Table 2. The mean composition, that is, $Au = 80.5\%$, $Ag = 15\%$, and $Cu = 4.5\%$, is quite similar to the mean composition of the gold areas of nose decorations.

Only the eight needles on bulk gold-alloy have different composition and are poor on silver and rich on copper, probably because of their use.

Transmission measurements

Attenuation measurements were carried out by using the equipment described in Section 2 with a secondary target on Sn. Results

Figure 17. Front and back sides of the nose decoration PACEB-F4-00018. It is composed of a body on laminated gold alloy showing two sneak's heads, a human figure on silver alloy, and, hanging on the gold structure, 12 disks on silver. The red line shows the position of quantitative grey-value curves from radiographs (Fig. 23). Gold alloy composition: *Au* = 75%, *Ag* = 20%, *Cu* = 5%. Silver alloy composition: *Ag* = 86.5%, *Cu* = 9.5%, *Au* = 4%.

are summarized in Table 3. The purpose of these measurements was to compare the results obtained with EDXRF-analysis, which is a surface analysis, with transmission measurements, which give a volume analysis, when the thickness of the examined object is known.

Radiography

Radiographs of nose decoration PACEB-F4-00002, 00106, and 00018 are shown (Figs 19–22). The radiography of the left-upper side indicates that the huts are glued to the gold body. The same is valid for the two shields.

Quite different is the situation concerning legs and feet, which appear black in the image (Fig. 15). The attenuation is similar to that of the gold body, and EDXRF-analysis exhibits a quite similar spectrum. The feet are, therefore, on gold alloy, and areas appearing blacker in the photo are less absorbent in the radiography. The gold sheet has a possibly decreasing thickness from legs to feet.

The case of nose decoration PACEB-F4-00106 is different, and fractures and soldering areas could be identified by radiographs.

Still different is the situation of nose decoration PACEB-F4-00018, in which gold and silver areas are attenuated in a similar manner, as can be observed by the radiographs. The suspect is that a unique layer of silver could be subject to aq process of depletion gilding.

Table 1. Composition of Au-areas of nose decorations N.2–34 and 102–112

Number PACEB-F4	Au(%)	Ag(%)	Cu(%)
2 (Fig. 16)	74.5	19.5	5.5
3	79.5	16	5.5
4	82	14.5	3.5
6	77	18.5	4.5
7	80.5	15.5	4
8	72	24	4
9	79	18	3
10	78	18.5	3.5
11	81	13.5	5.5
13	78	19	3
14	78	18	4
15	75.5	20.5	4
16	79.5	16	4.5
17	78.5	16.5	5
18 (Fig. 18)	75	20	5
19	78	17	5
20	82.5	14	3.5
21	80	15.5	4.5
22	77	17	6
23	82	14.5	3.5
24	75	21	4
25	80	16	4
26	80	15	5
27	74.5	20	5.5
28	74.5	23	2.5
29	82	12.5	5.5
30	80	14	6
31	80	14	6
32	77	18	5
33	81	17	2
102	82.5	13	4.5
103	80	14	6
104	85.5	11.5	3
105	80	14.5	5.5
106 (Fig. 17)	81.2	17.2	1.6
107	72.7	24.5	2.8
108	82.5	12.5	5
109	80.2	13.5	6.3
111	81.3	14.3	4.4
112	81	13.5	6.5
Mean value	79 ± 3	16.6 ± 3.2	4.4 ± 1.2

Optical microscopy

Typical Image from nose decoration PACEB-F4-00002 is shown in Fig. 23.

Silver

Energy-dispersive X-ray fluorescence-analysis

Image of a nose decoration, with gold and silver areas, is shown in Fig. 24. Results of EDXRF-analysis on all nose-decorations are shown in Table 4; the composition variety of the 41 nose decorations is very high. The not casual massive presence of Au in these Ag-alloys is not questionable and is very peculiar. It is possibly due to the purpose of limiting Ag-oxidation processes, or to give a special color to the Ag-alloy, or to some undetected processes of depletion gilding.

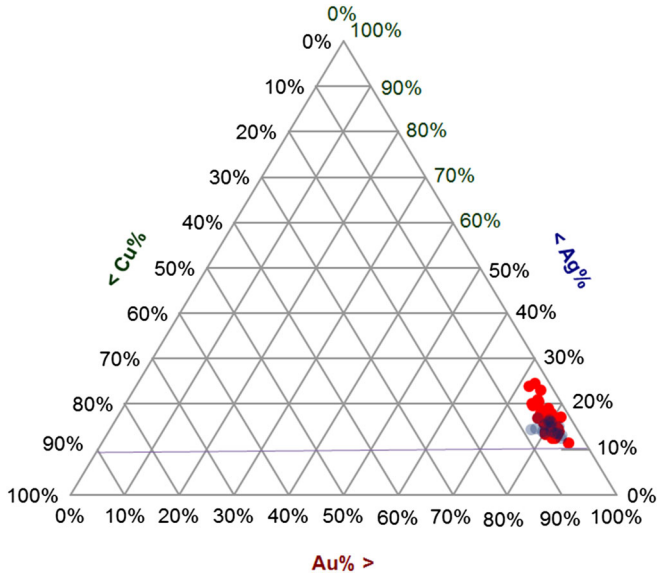

Figure 18. Distribution of gold, silver, and copper concentration for 41 nose decorations of the Lady of Cao. In red and black decorations from 2 to 34, and from 102 to 112, respectively.

Table 2. Analysis of 16 artifacts on gold

Object number*	Au(%)	Ag(%)	Cu(%)
PACEB-F4-0048	81	14	5
49-ear ring	82	13.5	4.5
50-ear ring	79.5	16	4.5
51-ear ring	79.5	16.5	4
54-ear ring	83.5	12.5	4
55-ear ring	82.5	13.5	4
56-ear ring	78	14.5	7.5
57-ear ring	77.5	14.5	8.5
58-ear ring	79	15.5	5.5
59-ear ring	79.5	14	6.5
71-dish	83.5 ± 1	13 ± 1	3.5 ± 0.5
89-necklace	80	13.5	6.5
90-necklace	80	16	4
91-necklace	80.5	15	4.5
94-necklace	77	17	6
95-necklace	82	15	3
Mean value	80.5 ± 2.0	15 ± 1.5	4.5 ± 2.0

Further, seven small heads on silver were analyzed, showing the following mean composition: *Ag* = 99%, *Cu* = 1%, and *Au* = 0.2%. However, the heads are completely oxidated, and the EDXRF-analyses could give only approximate results.

Transmission measurements

Results on transmission measurements of several nose decorations on silver areas are shown in Table 5, assuming that the results from EDXRF-analysis are reliable.

Further, the silver ear ring PACEB-F4-00060 was carefully examined by transmission measurements. This ear-ring is peculiar, because as many other objects from the tomb of the Lady of Cao is characterized by a very high gold content. Transmission measurements are able to verify if the strange composition of this ring

Table 3. Results of attenuation measurements on gold areas of nose decorations from the tomb of the Lady of Cao, partially on gold, and partially on silver

PACEB-F4-N.	d_{Au} (μm)*	d_t (μm)^
2 (Fig. 16)	100	120
3	180	210
6	155	200
8	65	200
10	140	170
11	110	110
12	140	140
13	100	335
17	120	195
20	135	205
23	120	205
29	175	140
Approximate mean values	130	185

* from attenuation measurements and Eqns (6') and (7').
^ from geometrical measurements (direct measurement or from mass and sizes; a direct measurement of thickness can give a partially erroneous result because of the non-flat surface and the previous use of a protective layer).

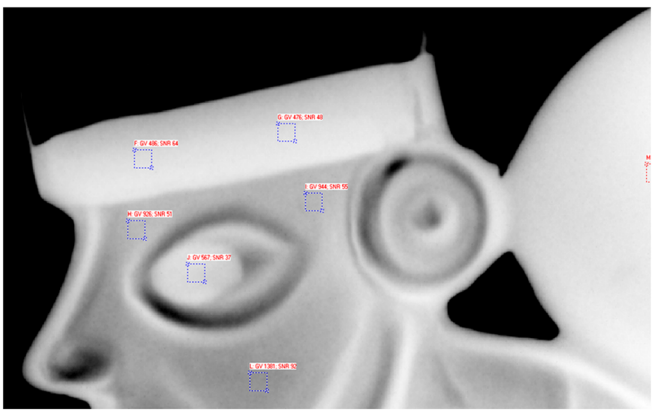

Figure 19. Radiography of the left-upper side of the nose-decoration PACEB-F4-0002 (Fig. 15) carried out at kV (to visualize the gold-layer). The thickness inhomogeneity is clearly represented by the gray levels and red numbers.

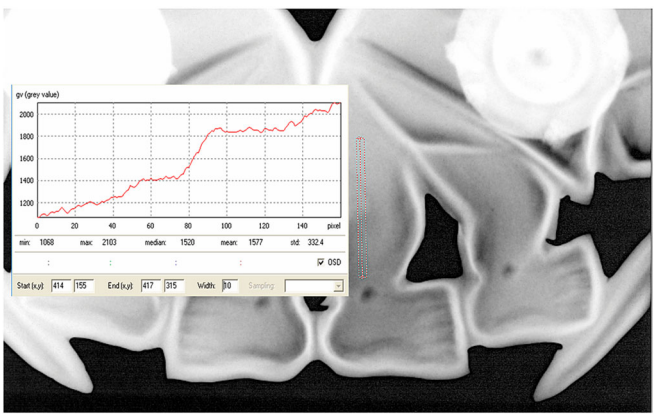

Figure 20. Radiography of the feet of nose-decoration PACEB-F4-0002. The feet are on gold alloy; areas appearing black in the photo (Fig. 15) exhibit quite similar EDXRF-spectra but appear less absorbent in the radiography. The gold sheet has a possibly slowly decreasing thickness *versus* feet.

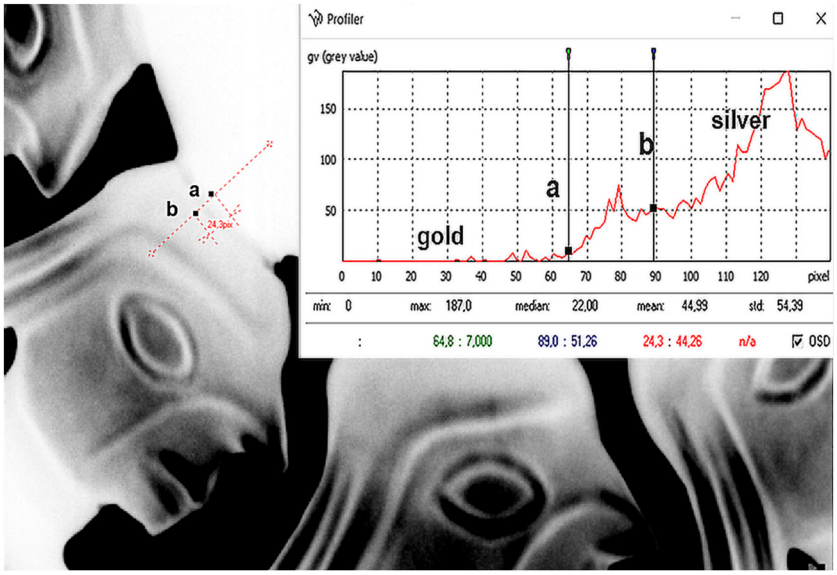

Figure 21. Radiography of first Ag-head on the right for nose decoration F4-00106, (last Ag-head and the gold strip, Fig. 18). In the enclosed curve, the interfaces are shown between the head and the gold structure (red vertical line). A possible interpretation of these interfaces is depicted in the red dashed line (in the image) and shown in the graphic: starting from the top (left in the graphics), we have an Ag-area of the head; then the discontinuity between Ag and soldering (the soldering covers partially the silver neck, and partially the gold strip), and then the gold region.

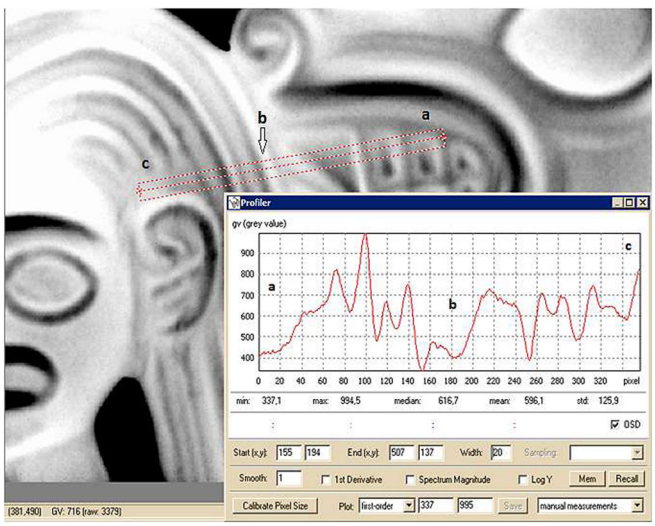

Figure 22. Radiography of nose decoration PACEB-F4-00018 (Fig. 17). It shows that the body supposed on laminated gold alloy and the human figure supposed on silver-alloy have similar mean grey values (blue lines). A possible hypothesis could be that a unique sheet on silver-alloy was employed and a gilding procedure was carried out on this alloy, on areas appearing as gold. This hypothesis requires confirmation.

Figure 23. Optical microscopy image of the back side of the nose decoration PACEB-F4-0002 (Fig. 15), which shows residual material at the interface between gold and silver laminas.

determined by EDXRF-analysis, that is, 48% Ag, 28% Cu, and 24% Au [and this strangeness is common to many other silver areas (Table 4)], could be related to the whole volume or the ring was affected by surface enrichment processes. The transmission measurements completely confirmed the EDXRF results.

Radiography

Figure 25 shown radiographic images of the silver hut of nose decoration PACEB-F4-00002, carried out at 25 kV (to imagine silver) and 50 kV (to imagine gold). In the bottom figures, is visible the area where gold and silver are glued.

Figure 26 shows the ear ring PACEB-F4-00060, which composition is shown in Table 7, and radiography in the same Fig. 26.

Gilded copper

Twenty-five objects from the tomb of the Lady of Cao are on gilded copper and are well preserved, because of the very dry atmosphere in the tomb and around it. The situation is different for the objects from the tombs of Sipán: among the many analyzed objects, not many were on gilded copper. The reason for that is the damp atmosphere in the tomb, which favors the corrosion processes that tends to destroy the gilding. For the same reason, gilded copper objects

Figure 24. Nose decoration PACEB-F4-00017 on gold and silver scorpions solded on a Au-Ag basis. The silver-alloy composition is: *Ag* = 64%, *Cu* = 16%, *Au* = 20%.

are generally well recognized, because of the many areas without residual gold.

Energy-dispersive X-ray fluorescence analysis

Table 6 shows the results of the 25 objects on gilded copper. The gold-leaf thickness is indicated the gilding composition, supposing that Cu is absent in the gilding (it is almost impossible to differentiate the possible presence of Cu in the gilding from the Cu-substrate). A mean gilding thickness of about 0.6 μm was measured, and a gold concentration of about 92%.

A clear comparison with other Moche artifacts on gilded copper is difficult, because of the very poor preservation of these other artifacts. However, in the few cases where this comparison is possible, the results agree with those of the 'Lady of Cao' artifacts.

Tumbaga

According to our measurements, there is no evidence of Cu-Au tumbaga in the pre-Moche cultures. At the contrary, there are many examples of tumbagas in the Moche culture.

Concerning the calculations of 'equivalent gold thickness'and composition of tumbaga, the first parameter can be evaluated through the ratios Cu(Kα/Kβ), Au(Lα/Lβ), and Au-Lα/Cu-Kα; for example, for the necklace 00088, these have the following values:

$$\mathrm{Cu(K}\alpha/\mathrm{K}\beta) = (0.73 \pm 0.05) \text{ corresponding to}$$
$$\mathrm{d} = (3.4 \pm 0.8)\ \mu\mathrm{m}$$

$$\mathrm{Au(L}\alpha/\mathrm{L}\beta)\ \mathrm{Au(L}\alpha/\mathrm{L}\beta) = (0.80 \pm 0.02) \text{ corresponding to}$$
$$\mathrm{d} = (6.5 \pm 1.7)\ \mu\mathrm{m}$$

$$\mathrm{Au} - \mathrm{L}\alpha/\mathrm{Cu} - \mathrm{K}\alpha = (2.2 \pm 1.0) \text{ corresponding to}$$
$$\mathrm{d} = (5.5 \pm 0.7)\ \mu\mathrm{m}.$$

Regarding composition, in the case of tumbaga, EDXRF-analysis is only giving an approximate indication, because the behavior of Au, Ag, and Cu concentration changes *versus* depth as shown, for example, in Figs 11 and 12.

Table 4. Composition of Ag-areas for nose decorations 2–33 and 102–112 and for other artifacts

PACEB F4-N.	Ag(%)	Cu(%)	Au(%)	Additional elements
2	99.2	0.02	0.8	Pb 0.2%
3	83	7.5	9.5	As 0.5%, Fe
4	92	4.5	3.5	area4.1, Hg ~ 0.4% (traces of Fe, Zn)
5	80	10	10	Pb 0.1–0.2%
6	91.5	4	4.5	Pb 0.2–0.4%
7	87	5	8	Pb 0.15–0.3%
8	41	25	34	—
9	79.5	13.5	7	—
10	52	21	27	—
11	64	21	15	—
12	45.5	35.5	19	—
13	85.5	10.5	4	—
14	51	25	24	—
15	61.5	14.5	24	—
16	73.5	13.5	13	—
17	64	16	20	Pb 0–0.15
18	86.5	9.5	4	Pb 0–0.4%
19	88	4	8	—
20	77	21	2	As 0.5–1%, Pb 0–0.1%
21	65.5	33.5	1	As or Pb 0.2%, Fe
22	71.5	14	14.5	Pb < 0.1%
23	76	11.5	12.5	—
24	61.5	25.5	13	Pb 0.2%, Fe
25	55.5	22	22.5	—
26	77	13.5	9.5	—
27	81.5	14.5	4	Pb 0.2%, Fe
28	89	7.5	3.5	Pb 0.3%
29	57.5	25.5	17	—
30	56.5	26	17.5	—
31	53.5	24	22.5	—
32	63.5	13	23.5	—
33	74.5	15.5	10	Pb 0.1%
34-ear ring	83.5	4.5	12	—
102-	82.1	4.4	13.5	—
102 ring	68	5.3	26.7	—
103	78.2	11.8	10	—
104	82.6	9.8	7.6	—
105	58.8	15.2	26	—
106	91.8	4.0	4.2	Pb
107	74.5	5.5	20	—
110	41.2	37.3	21.3	—
111	70.6	26.1	3.3	As, Pb
112	58.5	18.7	22.8	—
60-ear ring	48	28	24	—
61-ear ring	48	28	24	—
62-ear ring	76	14	10	—
63-ear ring	69	23	8	—
90-necklace	75	10.5	14.5	—

Energy-dispersive X-ray fluorescence analysis

Only five objects from the tomb of the Lady of Cao are supposed to be on tumbaga, according to the ratio (Au-Lα/ Cu-Kα) ~ 1;a nice collar with the figure of 12 human heads is shown in Fig. 27.

Table 5. Transmission measurements of silver areas for several nose decoration

PACEB-F4-N.000NN	SnKα/SnKα$_0$	SnKβ/SnKβ$_0$	d_{Ag}(μm)*
2 (huts)	0.18	0.0026	155
3 (upper rectangle)	0.013	0.0008	275
6 (bottom area)	0.07	0.00045	249
8 (head of right prawn)	0.0047	0.0004	166
10 (body of iguana)	0.035	0.005	125
11 (left side on the middle)	0.12	0.018	85
12 (half moon area)	0.016	0.0021	177
13 (half moon area)	0.009	low statistics	358
17 (upper right area)	0.007	0.0008	240
20 (body of animal on the left)	0.04	0.0006	275
23 (tail of the snake)	0.016	0.001	250
29 (bottom on the right) bottom	0.08	0.017	115

* from attenuation measurements and Eqns (6′) and (7′)

Table 7 shows the results giving the 'equivalent gold thickness', which is the Au-thickness producing the same effect of the tumbaga. A mean equivalent gilding thickness of about 3.4 μm was determined, and a Au-concentration of about 82%.

At the contrary, a large part of the artifacts from the Royal Tomb of Sipán is on tumbaga,[63,64] and the EDXRF-analysis gave the following mean results: Au-thickness = 2.3 ± 0.5 μm and Au-mean concentration = 87%.

Discussion and conclusions

Gold alloy artifacts

Following Caley,[65] native gold contains a moderate proportion of silver (up to about 30%) and a low proportion of copper (up to about 5%). Gold alloys of moderate to high fineness do not corrode, and therefore, the problem of their EDXRF-analysis is not complicated by the presence of corrosion products. Very poor gold alloys, especially when the alloying metal is copper, may corrode under natural conditions.

From the gold artifacts or gold areas from the tomb of the Lady of Cao (Tables 1 and 2), it appears evident that they have all a similar composition, that is,41 nose decorations, $Au = (79 \pm 3)\%$, $Ag = (16.6 \pm 3.2)\%$, $Cu = (4.4 \pm 1.2)\%$,; 16 other artifacts, $Au = (80.5 \pm 2)\%$, $Ag = (15 \pm 1.5)\%$, $Cu = (4.5 \pm 2)\%$, and; All artifacts, $Au = (79.5 \pm 2.5)\%$, $Ag = (16 \pm 2.5)\%$, $Cu = (4.5 \pm 1.5)\%$.

It is not usual to find such an homogeneous composition among artifacts from the same tomb.[63]

These values are, more or less, compatible with the hypothesis that the Moche from the time of the Lady of Cao (~300 AD) basically used native gold. However, composition of native gold varies greatly, not only from one deposit to another but also even within grains from the same deposit.[66] A possible explanation would be that the Moche knew how to mix Au, Ag, and Cu to produce gold objects of similar composition.

Silver alloy artifacts

Silver objects from early civilizations are scarce, apparently because they were always made from the scarce native metal. At first, the nearly pure metal was used without the addition of any alloying metal. Later, its alloys with copper were used to a greater extent. Impurities of Fe, Pb, Sn, Ni, and Au are often present in native silver.[65]

Energy-dispersive X-ray fluorescence analysis of silver areas of the 41 nose decorations shows that they have a completely erratic composition. Further, silver areas of the same object also exhibit an inhomogeneous composition. There is a reasonable suspect that at least some of them were subject to a depletion gilding process.

Silver from the tomb of the Lady of Cao (except for the seven small heads) is characterized by the presence of relatively high concentration of Au (up to about 37%) and Cu (up to about 37%). The presence of Au in silver alloys is common, but only at levels of traces. For example, silver artifacts from the tombs of Sipán are characterized by the systematic presence of Au, but at levels of percent. The small heads from the tomb of the Lady of Cao have about 99% silver, and that demonstrates that the Moche from Cao intentionally added Au and Cu to the silver alloy for unknown reasons. Why the Moche from the time

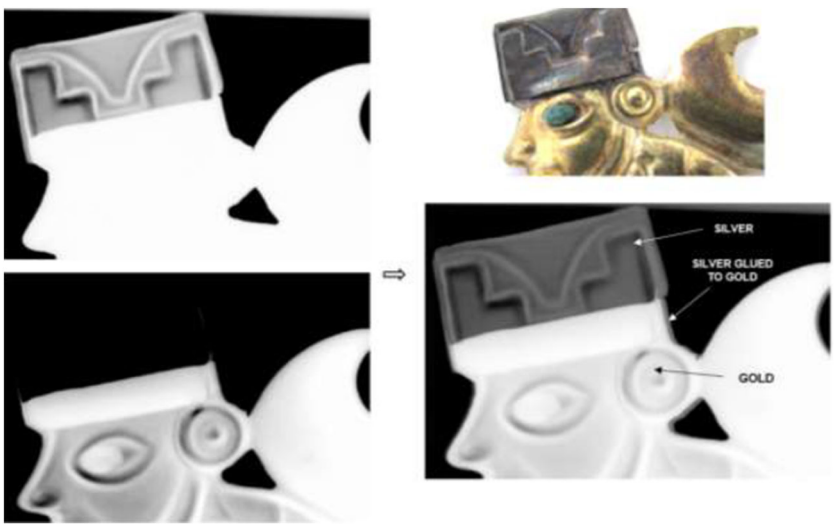

Figure 25. Radiographs of the nose decoration PACEB-F4-00002 (see Fig. 15 and image at top right). The radiography on the left top was carried out at 25 kV (to visualize the silver hut), on the left bottom at 50 kV (to visualize the gold figure). The image on the right bottom was obtained after an image processing from the two radiographic images on the left.

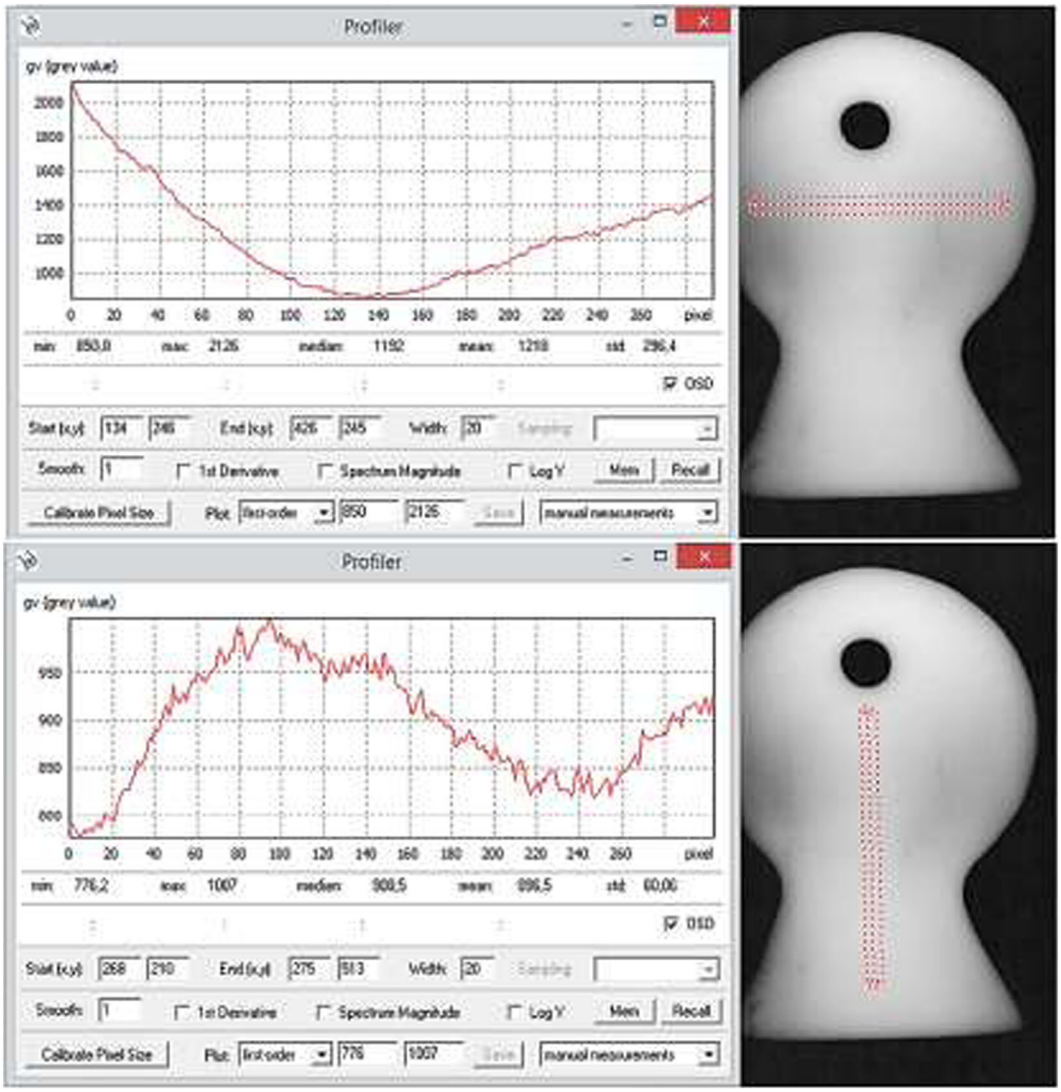

Figure 26. Radiographs of ear-ring F4-0060 and grey values along the red dashed horizontal line (top curve from right to left) and along the red dashed vertical line, from top to bottom. Gray values are logarithmically related to thickness differences, which are of the order of 10–15%.

of the Lady of Cao mixed high quantities of gold to the silver alloy is not clear; may be to give to the silver a luminous aspect or to limit the oxidation process?

Gold–silver junction of the nose decorations

The combination of gold and silver sheet is common among the artifacts from the tomb of the Lady of Cao, even if almost completely limited to nose ornaments. As observed by D. Schorsch for Moche artifacts from Loma Negra,[8] *it is clear that the visual juxtaposition of silver and gold was highly significant to the Moche.*

Concerning the junction between the two metals, this point is discussed by D. Schorsch, who identified three different methods as follows: (1) mechanical joining, (2) mechanical joining but with Cu-gilded or silvered, and (3) adhesive joining methods.

The radiographic images show that adhesive joining (possibly using natural resins) and soldering were employed by the Moche to produce gold–silver nose decorations. The solder should be, therefore, an alloy composed of one or more of the three metals, with high probability a silver alloy.

Copper-gold tumbaga

Poor Au-alloys enriched at the surface by depletion gilding (called by the Hyspanic 'tumbaga') are very common in pre-Columbian cultures, even if a few examples are also found in other ancient cultures. 'Tumbaga' gold was differentiated from a gold alloy from the altered Cu($K\alpha/K\beta$) and Au($L\alpha/L\beta$)-ratios. Concerning the presence of tumbaga in the Moche culture, the following may be observed from the analyzed objects.

Only five objects from the tomb of the Lady of Cao are supposed to be on tumbaga (Table 7), according to the ratio (Au-$L\alpha$/ Cu-$K\alpha$) ~ 1. A mean equivalent gilding thickness of about 3.4 μm was determined, and a Au-concentration of about 82%.

Artifacts on gilded copper

Twenty-five objects from the tomb of the Lady of Cao are on gilded copper and are generally well preserved because of the very dry atmosphere in the tomb.

Table 6 shows the results of the 27 objects on gilded copper from the tomb of the Lady of Cao. Supposing that Cu is absent in the

Table 6. Gold thickness and approximate composition* for 27 gilded copper objects from the tomb of the Lady of Cao

Object PACEB-F4-N.	d(μm)	Au(%)	Ag(%)
Pendant 00037	0.7	89	11
Pendant 00045	0.85	82	18
Pendant 00052	1.3	93	7
Pendant 00053	1.3	93.5	6.5
Diadem 00064	0.5	91	9
Diadem 00065	0.68	88	12
Diadem 00066	0.38	90	10
Diadem 00067	0.37	86	14
Crown 00068	0.85	89	11
Crown 00069	0.45	82	18
Crown 00070	0.7	89	11
Dish 00072	1.15	92	8
Dish 00073	0.9	90.5	9.5
Pendant 00099	0.3	100	0
Pendant 00101	1.1	57	43
Spear I1-00002	0.3	100	0
Spear I1-00003	0.5	100	0
Spear I1-00004	0.4	100	0
Spear I1-00005	0.4	100	0
Spear I1-00006	0.4	100	0
Spear I1-00007	0.5	100	0
Spear I1-00008	0.8	100	0
Spear I1-00009	0.95	88	12
Stick I1-00010	0.45	78–95.5	14 (4.5–22)
Stick I1-00011	0.43	88	12 (8.5–17)
Tissue with sheets PACEB-H1-00014	0.5	86	14
Tissue with sheets PACEB-H1-00015	0.55	88	12
Mean value	0.65 ± 0.3 μm	88**	12

* the composition was calculated in the hypothesis of absence of copper in the gilding.

** excluding the spears, which were analyzed with a Si-PIN detector having low efficiency for Ag.

Figure 27. Necklace PACEB-F4-00088 with 12 big heads on tumbaga.

Table 7. Gold thickness and 'equivalent gilding'composition for the five tumbaga objects

PACEB-F4-N.	d(μm)	Au(%)	Ag(%)	Cu(%)
35- ear ring	5.5 ± 1.0	65	15	20
36- ear ring	5.5 ± 1.0	65.5	15.5	20
46- pendant	6.0 ± 1.5	63.5	14.5	22
47- pendant	6.0 ± 1.0	64.5	14.5	21
88-necklace	6.0 ± 1.0	70	12.5	17.5
Mean value	5.7 ± 1.0	65.5 ± 2.5	14.5 ± 1.0	20 ± 1.5

gilding, a mean gilding thickness of about 0.6 μm was measured, and a gold concentration of about 92%.

A clear comparison with other Moche artifacts on gilded copper is difficult, because of the very poor preservation of these other artifacts. However, in the few cases where this comparison is possible, the results are not very different from those of the 'Lady of Cao' artifacts.

Trace elements

With regard to detection of trace elements, it should be observed that EDXRF in the employed portable version is not able to detect trace element with atomic number $Z < 18$. Further, it may be observed that gold alloys are relatively free from trace elements, with the exception of Fe and Zn (this last element only in Sipán gold), while in silver alloys and in copper, they are present trace elements such as Fe, Ni, Zn, As, Br, and Pb. More specifically, the following may be observed.Iron, – this element is often present in the Moche alloys and was detected in many artifacts from the tomb of the Lady of Cao (Table 4).; Zinc, – this element is often present in Sipán alloys but only in one case, it was detected in artifacts from the tomb of the Lady of Cao.; Arsenic, – this element was never detected before the period of the Moche culture. It was detected sometimes in silver from the tomb of the Lady of Cao (Table 4). The following the literature is typically present in ancient copper objects, sometimes at levels higher than 4–5% (arsenical bronze).[65]; Mercury, – among the Cao artifacts, this element was only clearly detected in the silver area n.1 of artifact PACEB-F4-0004 .; Lead, – lead, which is a relatively common element in silver alloys, was detected at level of traces in many silver objects from Cao (Table 4).; Platinum, – this element, systematically detected in pre-Columbian gold from Equador (63), is difficult to detect and identify by EDXRF-analysis because its L-lines are close to those of Au. Only an enlargement of Au-Lβ may be expected for Pt-concentrations lower than 5% approximately, and this enlargement was never observed.

Acknowledgements

This work was partially supported by the Consiglio Nazionale delle Ricerche first, in the framework of the Progetto Finalizzato 'Beni Culturali' and then, by the bilateral project between the Consiglio Nazionale delle Ricerche and Consejo Nacional de Ciencia, Tecnologia e Innovacion Tecnologica of Perù (CNR-CONCYTEC, 2009–2011).

The 'Fundacion Wiese' is acknowledged for permitting to analyze the artifacts from the tomb of the Lady of Cao and for encouraging this research.

Dr Stefano Ridolfi is acknowledged for providing several 'Tarì' standard samples of gold alloys, and for useful discussions.

J. Fabian expresses their gratitude to the International Centre for Theoretical Physics Abdus Salam, for a 5-month grant at the University of Sassari.

Lorenzo Manetti, of the firm 'Giusto Manetti', Florence, Italy, is acknowledged for providing standard gold samples.

Luciano Mastrolorenzi, distinguished sculptor and goldsmith, is acknowledged for many discussions about Moche metallurgy and for preparing gold and silver samples of Moche imitation.

Prof. Emma Angelini and Dr Sabina Grassini from the Polytechnic of Turin are acknowledged for preparing samples of gilded copper with calibrated Au-thickness.

Renato Pereira de Freitas from COPPE, Universidade Federal do Rio de Janeiro, Rio de Janeiro, Brasil, contributed with measurements.

Marcia Rizzutto, Instituto de Fisica, Universidade de São Paulo, SP, Brasil, contributed with measurements and suggestions.

Fabio Lopes Instituto de Fisica, Universidade de Londrina, PA, Brasil, contributed with measurements.

References

[1] W. Alva, *SIPAN, Descrubrimiento y Investigation*, Quebecor World Perù S. A, Lima, **2004**.
[2] W. Alva, C. B. Donnan, *The Royal Tomb of Sipán*, Los Angeles Fowler Museum of Cultural history, University of California, Los Angeles, **1993**.
[3] R. Franco Jordan, in *Señores de los Reinos de la Luna*, (Ed: K Makowski), Banco de Crédito del Perù, Lima, **2008**, pp. 280–287.
[4] R. Franco Jordan, *Los Secretos de la Huaca Cao Viejo*, Fundacion Wiese y Petrolera Transoceanica S.A., Lima, **2009**.
[5] R. Franco Jordan, *Pour la Science*, Paris, France, **2010** 8, pp. 390.
[6] R. Franco Jordan, La Dama de Cao, in *Investigacion y Ciencia*, Bercelona, Spain, **2011**, pp. 68–74.
[7] H. Lechtman. *American Antiquity* **1998**, *47*(1), 3.
[8] D. Schorsch. *Metropolitan Museum Journal* **1998**, *33*, 109.
[9] G. Hőrz, G. And, M. Kallfass. *JOM* **1998**, *50*, 8.
[10] G. Hőrz, M. Kallfass. *Mater Charact* **2000**, *45*, 391.
[11] A. Galli, L. Bonizzoni, E. Sibilia, M. Martini. *X-Ray Spectrometry* **2011**, *40*(2), 74.
[12] H. Lechtman. *Sci. Am.* **1984**, *250*, 38.
[13] J. L. Ruvalcaba Sil, *X-Rays for Archaeology*, Springer Netherlands, Amsterdam, **2001**, pp. 123–149.
[14] W. Bray, Techniques of gilding and surface enrichment in pre-Hispanic American metallurgy in *Metal Plating and Platination*, (Eds: S. La Niece, P. Craddock), Butterworth-Heinemann, **1993**, pp. 182–192.
[15] D. A. Scott, A review of gilding techniques in ancient South America in *Gilded Metals: History, Technology and Conservation*, (Eds: T. Drayman-Weisser) Archetype Publ, London **2000**, pp. 203–222.
[16] E. Andrade, A. Romero Nunez, A. Ibarra Palos, J. Cruz, M. F. Rocha, C. Solis. *Nuclear Instrum Methods in Phys. Res. B* **2005**, *240*, 570.
[17] R. Cesareo, C. Calza, M. Dos Anjos, R. T. Lopes, A. Bustamante, J. Fabian, W. Alva, L. Chero. *Appl. Radiat. Isot.* **2010**, *68*, 525.
[18] S. La Niece. *Ur. Iraq* **1995**, *57*, 41.
[19] C. Fraresso. *Boletín del Instituto de Estudios Franceses* **2010**, *39-2*, 351.
[20] J. C. Tello. *American Antiquity* **1943**, *9*(1), 135.
[21] R. L. Burger, *Chavin and the origins of Andean Civilization*, Thames and Hudson, New York, **1992**.
[22] R. L. Burger, Chavin de Huantar and its sphere of influence, in *Handbook of South American Archeology*, (Eds: H. Silverman, W. Isbell), Springer, New York, **2008**, pp. 681–706.
[23] J. Merkel, I. Shimada, C. P. Swann, R. Doonan, Pre-Hispanic copper alloy production at Batan Grande, Peru: interpretation of the analytical data for ore samples, in *Archaeometry of pre Columbian Sites and Artefacts*, (Eds: D. A. Scott, P. Meyers), The Getty Conservation Institute, Santa Monica, **1994**, pp. 199–227.
[24] C. B. Donnan, *Moche art of Peru. Pre-Columbian symbolic communication*, Fowler Museum of Cultural History, University of California, Los Angeles, **1978**.
[25] H. Lechtman. *Technol. Cult.* **1984**, *25*, 1.
[26] H. Lechtman, Traditions and styles in central Andean metalworking, in *The Beginning of the use of the Metals and Alloys*, (Ed: R. Maddin), MIT Press, Cambridge, MA, **1988**, pp. 344–378.
[27] J. Jones, Mochica works of art in metal: a review, in *Pre-Columbian metallurgy of South America*, (Ed: E. P. Benson), Dumbarton Oaks Research Library and Collections, Trustees for Harvard University, Washington DC, **1979**, pp. 53–104.
[28] H. Lechtman. *J. Field Archaeol.* **1991**, *18*, 45.
[29] P. C. Muro, I. Shimada, Behind the golden mask. Sican gold artifacts from Batan Grande, Peru in *The Art of Pre-Columbian gold. The Jan Mitchel Collection*, (Ed: J. Jones), Weidenfeld and Nicolson, London, **1985**, pp. 61–67.
[30] W. Alva. *Nat. Geosci.* **1988**, *174*, 550.
[31] W. Alva, M. Fecht, P. Schauer, M. Tellenbach, *Das Fürstengrab von Sipan, Entdeckung und Restaurierung*, Verlag des Römisch-Germanischen Zentralmuseums, Mainz, Germany, **1989**.
[32] H. Lechtman. *J. Appl. Meteorol.* **1979**, *31*, 154.
[33] H. Lechtman. *Sci. Am.* **1984**, *250*, 38.
[34] Y. Hirao, J. Ohnishi, Y. Onuki, Y. Kato. Chemical composition of samples excavated from Kuntur Wasi archaeological site, Peru. *Archaeology and Natural Science* **1992**, *25*, 13–30 in Y. Onuki and K. Inokuchi: El Tesoro del temple de Kuntur Wasi; Fondo Editorial del Congreso del Peru; Quadgraphics Peru: Lima **2011**.
[35] S. Schlosser, A. Kovacs, E. Pernicka, D. Günther, M. Tellenbach. Fingerprints in gold in *New Technologies Multidisciplinary Investigations in Palpa and Nasca, Peru*, (Eds: M. Reindel, G. A. Wagner), Springer Verlag, Berlin, Heidelberg, **2009**.
[36] S. Izumi, *The Late Prehispanic Coasted States in the Inca World. The Development of pre-Columbian Peru*, (Ed: L. Laurencich Minelli), Norman University of Oklahoma Press, Oklahoma City, **2000**, pp. 49–82.
[37] Nickle Arts Museum, *Ancient Peru Unearthed Golden Treasures of a Lost Civilization*, The Nickle Arts Museum, Calgary, **2006**.
[38] AMPTEK Inc., 6 De Angelo Drive, Bedford, MA 01730-2204, USA.
[39] R. Cesareo, A. Brunetti, A. Castellano, M. A. Rosales, Portable equipment for X-ray fluorescence analysis, in *X-ray Spectrometry: Recent Technological Advances*, (Eds: K. Tsuji, J. Injuk, R. Van Grieken), J. Wiley & Sons, Chichester, UK, **2004**, pp. 307–341
[40] R. Cesareo, X-ray physics in *La Rivista del Nuovo Cimento*, Ed. Compositori, Bologna, Italy, **2000**.
[41] A. Markowicz, X-ray physics in *Handbook on X-ray Spectrometry: Methods and Techniques*, (Eds: R. Van Grieken, A. Markowicz), M. Dekker Inc, New York, Basel, Hong Kong, **1992**, Chapter 1.
[42] R. Cesareo, A. Brunetti. *J. X-Ray Sci. and Techn.* **2008**, *16*(2), 119.
[43] B. Ertugral, G. Apayadin, U. Çevik, M. Ertugrul, Al. Kobya. *Radiation Phys. And Chem.* **2007**, *76*, 15.
[44] W. T. Elam, B. D. Ravel, J. R. Sieber. *Rad. Phys. And Chem.* **2002**, *63*, 121.
[45] T. Trojek, J. Wegrzynek. *Nucl. Instrum. Methods* **2009**, *A619*, 311.
[46] C. Neelmijer, I. Brissaud, T. Calligaro, G. Demortier, A. Hautjärvi, M. Mäder, M. Schreiner, T. Truernala, G. Weber. *X-ray Spectrometry* **2000**, *29*, 101.
[47] J. H. Hubbell, W. J. Veigele, E. A. Briggs, R. T. Brown, D. T. Cromer, R. J. Howerton. *J. Phys. Chem. Ref. Data* **1975**, *4*, 471.
[48] C. Fiorini, M. Gianoncelli, A. Longoni, F. Zaraga. *X-Ray Spectrometry* **2002**, *31*, 92.
[49] R. Cesareo. *Nucl. Instrum. Methods in Phys. Res.* **2003**, *B211*, 133.
[50] R. Cesareo, M. A. Rizzutto, A. Brunetti. *Nucl. Instrum. Methods* **2009** B, *267*, 2890.
[51] N. Ekinci, E. Baydas, Y. Sahin. *Instrum. Sci. Technol.* **1999**, *27*, 181.
[52] M. Ferretti, C. Polese, C. Roldán Garcia. *Spectrochemica Acta* **2013** Part B, *83–84*, 21.
[53] A. C. Sparavigna, Depletion and Enrichment of an Alloy Surface; Archaeogate **2013**.
[54] S. La Niece, M. Cowell, Crimean Metalworking; Analysis and Technical Examination in the Berthier-Delagarde Collection of Crimean Jewellery in the British Museum, pp. 151–160.
[55] N. Foster, P. Grave, N. Vikery, L. Kealhofer. *X-ray Spectrom.* **2011**, *40*, 389.
[56] D. A. Scott. *Studies in Conservation* **1983**, *28*, 194.
[57] E. S. Blakelock. *Archaeometry* **2015** online version. 5 October 2015.
[58] M. Ferretti. *J. Anal. At. Spectrom.* **2014**, *29*, 1753.
[59] U. Bottigli, A. Brunetti, B. Golosio, P. Oliva, S. Stumbo, L. Vincze, P. Randaccio, P. Bleuet, A. Simionovici, A. Somogyi. *Spectroch. Acta* **2004** B, *59*, 1747.
[60] R. Cesareo. *X-ray Spectrometry* **2014**, *43*, 312.
[61] R. Cesareo. Work in Preparation **2015**.
[62] R. Cesareo, A. Bustamante, J. Fabian, S. del Pilar Zambrano Alva, R. Franco, A. Fernandez, G. Gigante. *Archeomatica settembre* **2015**, *6*–10.
[63] R. Cesareo, A. Bustamante, J. Fabian, Z. Sandra del Pilar, C. Calza, M. dos Anjos, R. T. Lopes, W. Alva, L. Chero, M. C. Espinoza Cordoba, R. G. Vasquez, R. R. Ruiz, M. S. Fernandez. *Appl. Rad. Isotopes* **2010**, *68*, 525.
[64] R. Cesareo, A. Bustamante, J. Fabian, S. del Pilar Zambrano, C. Calza, M. dos Anjos, R. T. Lopes, W. Alva, L. Chero, M. C. Espinoza Cordoba, R. G. Vasquez, R. R. Ruiz, M. S. Fernandez. *X-ray Spectrometry* **2011**, *40*, 37.
[65] E. R. Caley, *Analysis of ancient metals*, Pergamon Press, Oxford, London, New York, **1964**.
[66] *Geochemical Exploration 1976*, (Eds: C. R. M. Butt, I. G. P. Wilding), Elsevier Sci. Publ. Co., Amsterdam, **1977**.